

Holographic Thermalization, stability of AdS, and the Fermi-Pasta-Ulam-Tsingou paradox

Venkat Balasubramanian,^{1,*} Alex Buchel,^{1,2,†} Stephen R. Green,^{3,‡} Luis Lehner,^{2,§} and Steven L. Liebling^{4,¶}

¹*Department of Applied Mathematics, University of Western Ontario, London, Ontario N6A 5B7, Canada*

²*Perimeter Institute for Theoretical Physics, Waterloo, Ontario N2L 2Y5, Canada*

³*Department of Physics, University of Guelph, Guelph, Ontario N1G 2W1, Canada*

⁴*Department of Physics, Long Island University, Brookville, NY 11548, U.S.A*

For a real massless scalar field in general relativity with a negative cosmological constant, we uncover a large class of spherically symmetric initial conditions that are close to AdS, but whose numerical evolution does not result in black hole formation. According to the AdS/CFT dictionary, these bulk solutions are dual to states of a strongly interacting boundary CFT that fail to thermalize at late times. Furthermore, as these states are not stationary, they define dynamical CFT configurations that do not equilibrate. We develop a two-timescale perturbative formalism that captures both direct and inverse cascades of energy and agrees with our fully nonlinear evolutions in the appropriate regime. We also show that this formalism admits a large class of quasi-periodic solutions. Finally, we demonstrate a striking parallel between the dynamics of AdS and the classic Fermi-Pasta-Ulam-Tsingou problem.

Introduction.—The gauge theory-string theory correspondence [1] has become a valuable tool to study nonequilibrium phenomena in strongly interacting QFTs [2–4]. In a particular limit, this correspondence links general relativity in $d+1$ -dimensional asymptotically anti-de Sitter (AdS $_{d+1}$) spacetimes with d -dimensional conformal field theories. A question of particular importance in field theory is to understand the process of equilibration and thermalization. This corresponds, in the bulk, to collapse of an initial perturbation to a black hole.

In the first detailed analysis [5] of dynamics of perturbations of global AdS $_4$, Bizoń and Rostworowski argued that (except for special *nonresonant* initial data) the evolution of a real, massless, spherically symmetric scalar field *always* results in gravitational collapse, even for arbitrarily small initial field amplitude ϵ . At the linear level, this system is characterized by a normal mode spectrum with natural frequencies $\omega_j = 2j + 3$. Using weakly nonlinear perturbation theory, these authors described the onset of instability as a result of resonant interactions between the normal modes. Because of the presence of a vast number of resonances, they argued that this mechanism leads to a *direct turbulent cascade* of energy to high mode numbers, making gravitational collapse inevitable. Higher mode numbers are more sharply peaked, so this corresponds to an effect of gravitational focusing.

The analysis of [5] also showed that, for initial data consisting of a single mode, the dominant effect of resonant self-interaction could be absorbed into a constant shift in the frequency of the mode. (This time-periodic solution was confirmed to persist at higher nonlinear order [6].) However, for two-mode initial data, additional resonances are present that cannot be absorbed into frequency shifts. The result is secular growth of higher modes.

The turbulent cascade described in [5] is a beautiful mechanism for thermalization of strongly coupled QFTs

with holographic gravitational duals. However, it was recently pointed out that this cascade argument breaks down if *all* modes are initially populated, and the mode amplitudes fall off sufficiently rapidly for high mode numbers [7]. In this case, all resonant effects may once again be absorbed into frequency shifts and black hole collapse is avoided. Low-lying modes have broadly distributed bulk profiles. Thus, one might expect that if the initial scalar profile is broadly distributed, its evolution might not result in gravitational collapse (see also [8–10]). This prediction was verified numerically [11]. The physical mechanism responsible for collapse/non-collapse of small amplitude initial data is a competition between two effects: gravitational focusing and nonlinear dispersion of the propagating scalar field. If the former dominates, gravitational collapse ensues [5]. If the latter does, the system evolves without approaching any identifiable static or stationary solution—the perturbed boundary CFT neither thermalizes nor equilibrates at late times [11].

The perturbation theory of [5] cannot make predictions at late times. (The growth of secular terms in the expansion causes a breakdown at time $t \propto 1/\epsilon^2$.) It also does not properly take into account energy transfer between modes. In this Letter, we undertake a thorough analysis of the dynamics of AdS by making use of a new perturbative formalism for analyzing the effect of resonances on the evolution of this system *that is valid for long times*. We also perform fully nonlinear GR simulations (see [7, 11] for details of our numerical implementation and validation). In the process we uncover a close relationship between the dynamics of AdS and the famous Fermi-Pasta-Ulam-Tsingou (FPUT) problem [12, 13]. Our formalism is based on a two-timescale approach [14], where we introduce a new “slow time” $\tau = \epsilon^2 t$. The timescale τ characterizes energy transfers between modes, whereas the “fast time” t characterizes

the original normal modes. Importantly, this formalism allows one to study the system for long times and examine energy transfer between modes. In the following we describe the *Two Time Framework* (TTF) and determine a large class of quasi-periodic solutions that extends the single-mode periodic solutions of [5, 6]. These solutions have finely tuned energy spectra such that the net energy flow into each mode vanishes, and they appear to be stable to small perturbations within both TTF and full numerical simulations. We then study the behavior of two-mode initial data of [5] under both approaches. Finally, we use the TTF equations to draw an interesting parallel between scalar collapse in AdS and the FPUT problem of thermalization of nonlinearly coupled oscillators [12].

Model.—Following [5], we consider a self-gravitating, real scalar field ϕ in asymptotically AdS₄ spacetime. Imposing spherical symmetry, the metric takes the form

$$ds^2 = \frac{1}{\cos^2 x} (-Ae^{-2\delta} dt^2 + A^{-1} dx^2 + \sin^2 x d\Omega^2), \quad (1)$$

where we set the asymptotic AdS radius to one. Spherical symmetry implies that A , δ and ϕ are functions of time $t \in (-\infty, \infty)$ and the radial coordinate $x \in [0, \frac{\pi}{2})$.

In terms of the variables $\Pi \equiv e^\delta \dot{\phi}/A$ and $\Phi \equiv \phi'$, the equation of motion for ϕ is

$$\ddot{\phi} = \left(\dot{A}e^{-\delta} - A\dot{\delta}e^{-\delta} \right) \Pi + A^2 e^{-2\delta} \Phi' \quad (2)$$

$$+ \left(\frac{2}{\sin x \cos x} A^2 e^{-2\delta} + AA' e^{-2\delta} - A^2 e^{-2\delta} \delta' \right) \Phi,$$

while the Einstein equation reduces to the constraints,

$$A' = \frac{1 + 2 \sin^2 x}{\sin x \cos x} (1 - A) + \sin x \cos x A (|\Phi|^2 + |\Pi|^2), \quad (3)$$

$$\delta' = -\sin x \cos x (|\Phi|^2 + |\Pi|^2). \quad (4)$$

Two Time Framework.—TTF consists of defining the slow time $\tau = \epsilon^2 t$ and expanding the fields as

$$\phi = \epsilon \phi_{(1)}(t, \tau, x) + \epsilon^3 \phi_{(3)}(t, \tau, x) + O(\epsilon^5), \quad (5)$$

$$A = 1 + \epsilon^2 A_{(2)}(t, \tau, x) + O(\epsilon^4), \quad (6)$$

$$\delta = \epsilon^2 \delta_{(2)}(t, \tau, x) + O(\epsilon^4). \quad (7)$$

It is possible to go beyond $O(\epsilon^3)$ by introducing additional slow time variables. However, the order of approximation used here is sufficient to capture the key aspects of weakly nonlinear AdS collapse in the $\epsilon \rightarrow 0$ limit.

Perturbative equations are derived by substituting the expansions (5)–(7) into the equations of motion (2)–(4), and equating powers of ϵ . It is important to note that, when taking time derivatives of a function of both time variables we have $\partial_t \rightarrow \partial_t + \epsilon^2 \partial_\tau$. At $O(\epsilon)$, we obtain the wave equation for $\phi_{(1)}$ linearized off exact AdS,

$$\partial_t^2 \phi_{(1)} = \phi_{(1)}'' + \frac{2}{\sin x \cos x} \phi_{(1)}' \equiv -L\phi_{(1)}. \quad (8)$$

The operator L has eigenvalues $\omega_j^2 = (2j + 3)^2$ ($j = 0, 1, 2, \dots$) and eigenvectors $e_j(x)$ (“oscillons”) [5]. Explicitly,

$$e_j(x) = d_j \cos^3 x {}_2F_1 \left(-j, 3 + j; \frac{3}{2}; \sin^2 x \right), \quad (9)$$

with $d_j = 4\sqrt{(j+1)(j+2)}/\sqrt{\pi}$. The oscillons form an orthonormal basis under the inner product

$$(f, g) = \int_0^{\pi/2} f(x)g(x) \tan^2 x dx. \quad (10)$$

The general real solution to (8) is

$$\phi_{(1)}(t, \tau, x) = \sum_{j=0}^{\infty} (A_j(\tau)e^{-i\omega_j t} + \bar{A}_j(\tau)e^{i\omega_j t}) e_j(x), \quad (11)$$

where $A_j(\tau)$ are arbitrary functions of τ , to be determined later.

At $O(\epsilon^2)$ the constraints (3)–(4) have solutions

$$A_{(2)}(x) = -\frac{\cos^3 x}{\sin x} \int_0^x (|\Phi_{(1)}(y)|^2 + |\Pi_{(1)}(y)|^2) \tan^2 y dy, \quad (12)$$

$$\delta_{(2)}(x) = -\int_0^x (|\Phi_{(1)}(y)|^2 + |\Pi_{(1)}(y)|^2) \sin y \cos y dy. \quad (13)$$

Finally, at $O(\epsilon^3)$ we obtain the equation for $\phi_{(3)}$,

$$\partial_t^2 \phi_{(3)} + L\phi_{(3)} + 2\partial_t \partial_\tau \phi_{(1)} = S_{(3)}(t, \tau, x), \quad (14)$$

where the source term is

$$S_{(3)} = \partial_t (A_{(2)} - \delta_{(2)}) \partial_t \phi_{(1)} - 2(A_{(2)} - \delta_{(2)}) L\phi_{(1)} \quad (15)$$

$$+ (A'_{(2)} - \delta'_{(2)}) \phi'_{(1)}.$$

The solutions (12)–(13) for $A_{(2)}$ and $\delta_{(2)}$ are substituted directly into $S_{(3)}$. In general, the source term $S_{(3)}$ contains resonant terms (*i.e.*, terms proportional to $e^{\pm i\omega_j t}$). As noted in [5], for all triads (j_1, j_2, j_3) , resonances occur at $\omega_j = \omega_{j_1} + \omega_{j_2} - \omega_{j_3}$. In ordinary perturbation theory these resonances lead to secular growths in $\phi_{(3)}$. However, [5] showed that in *some* cases the growths may be absorbed into frequency shifts. TTF provides a natural way to handle these resonances by taking advantage of the new term $2\partial_t \partial_\tau \phi_{(1)}$ in (14) and the freedom in $A_j(\tau)$.

We now project (14) onto an individual oscillon mode e_j and substitute for $\phi_{(1)}$,

$$(e_j, \partial_t^2 \phi_{(3)} + \omega_j^2 \phi_{(3)}) - 2i\omega_j (\partial_\tau A_j e^{-i\omega_j t} - \partial_\tau \bar{A}_j e^{i\omega_j t}) \quad (16)$$

$$= (e_j, S_{(3)}).$$

By exploiting the presence of terms proportional to $e^{\pm i\omega_j t}$ on the left hand side of the equation, we may cancel off

the resonant terms on the right hand side. Denoting by $f[\omega_j]$ the part of f proportional to $e^{i\omega_j t}$, we set

$$-2i\omega_j \partial_\tau A_j = (e_j, S(t, \tau, x))[-\omega_j] = \sum_{klm} \mathcal{S}_{klm}^{(j)} \bar{A}_k A_l A_m, \quad (17)$$

where $\mathcal{S}_{klm}^{(j)}$ are real constants representing different resonance channel contributions. The right hand side is a cubic polynomial in A_j and \bar{A}_j . Thus, we have obtained a set of coupled first order ODEs in τ for A_j , which we shall refer to as the *TTF equations*. The equations are to be solved given the initial conditions for ϕ . This procedure fixes the arbitrariness in the solution (11) for $\phi_{(1)}$. While we could also solve for $\phi_{(3)}$, this would be of little interest since the lack of resonances remaining in (14) implies that $\phi_{(3)}$ remains bounded.

Under evolution via the TTF equations, both the amplitude and phase of the complex coefficients $A_j(\tau)$ can vary. Thus, in contrast to the perturbative analysis in [5], the energy per mode $E_j = \omega_j^2 |A_j|^2$ can change with time in a very nontrivial manner. However, it can be checked that the total energy $E = \sum_j E_j$ is conserved. TTF thus describes an energy-conserving dynamical system. The TTF equations also possess a scaling symmetry $A_j(\tau) \rightarrow \epsilon A_j(\tau/\epsilon^2)$. This symmetry was observed in Fig. 2b of [5], which indicates that the instability mechanism is captured by TTF.

In practice, it is necessary to truncate the TTF equations at finite $j = j_{\max}$. We evaluated $\mathcal{S}_{klm}^{(j)}$ up to $j_{\max} = 47$. In particular, under truncation to $j_{\max} = 0$, the equations reduce to

$$i\pi \partial_\tau A_0 = 153 A_0^2 \bar{A}_0, \quad (18)$$

with solution $A_0(\tau) = A_0(0) \exp(-i \frac{153}{\pi} |A_0(0)|^2 \tau)$. This reproduces precisely the single-mode frequency shift result of [5].

Quasi-periodic solutions.—To understand the dynamics of TTF, we first look for quasi-periodic solutions. For $j_{\max} = 0$ this is the periodic solution above. For general $j_{\max} > 0$ we take as ansatz $A_j = \alpha_j \exp(-i\beta_j \tau)$, where $\alpha_j, \beta_j \in \mathbb{R}$ are independent of τ . These solutions have $E_j = \text{constant}$, so they represent a balancing of energy fluxes such that each mode has constant energy. Substituting into the TTF equations, the τ -dependence can be canceled by requiring $\beta_j = \beta_0 + j(\beta_1 - \beta_0)$. This leaves $j_{\max} + 1$ algebraic equations,

$$-2\omega_j \alpha_j [\beta_0 + j(\beta_1 - \beta_0)] = \sum_{kmn} \mathcal{S}_{kmn}^{(j)} \alpha_k \alpha_m \alpha_n, \quad (19)$$

for $j_{\max} + 3$ unknowns $(\beta_0, \beta_1, \{\alpha_j\})$. The equations for $j = 0, 1$ may be used to eliminate (β_0, β_1) , leaving $j_{\max} - 1$ equations to be solved for $\{\alpha_j\}$ —two parameters of underdetermination. The scaling symmetry allows for elimination of one parameter, so we set $\alpha_{j_r} = 1$ for some fixed

$0 \leq j_r < j_{\max}$. Taking the remaining free parameter to be α_{j_r+1} and requiring solutions to be insensitive to the value of j_{\max} (*i.e.*, stable to truncation), it is straightforward to construct solutions perturbatively in $\alpha_{j_r+1}/\alpha_{j_r}$. We find a single solution for $j_r = 0$ and precisely two otherwise (see Fig. 1).

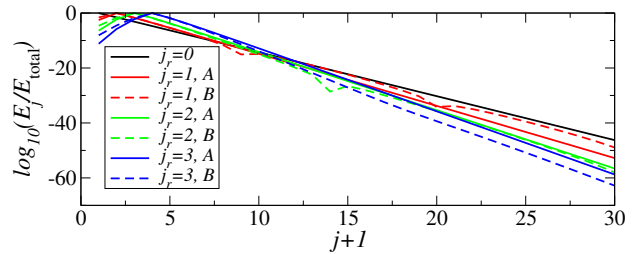


FIG. 1. Energy spectra of quasi-periodic solutions with $\alpha_{j_r+1}/\alpha_{j_r} = 0.1$ for $j_r = 0, 1, 2, 3$. Dashed and solid lines distinguish different branches for $j_r > 0$. The solid branch is well-approximated by an exponential to each each side of j_r . For $\alpha_{j_r+1}/\alpha_{j_r}$ too large, it becomes difficult to obtain solutions to (19), but for $j_r = 0$, we can go up to $\alpha_1/\alpha_0 \approx 0.42$. (Constructed for $j_{\max} = 30$.)

Stability of quasi-periodic solutions.—Ref. [6] extended single-mode, time-periodic solutions to higher order in ϵ and found these solutions to be stable to perturbations. Similarly, we examine the stability of our extended class of quasi-periodic solutions, both using full numerical relativity simulations and by numerically solving the TTF ODEs.

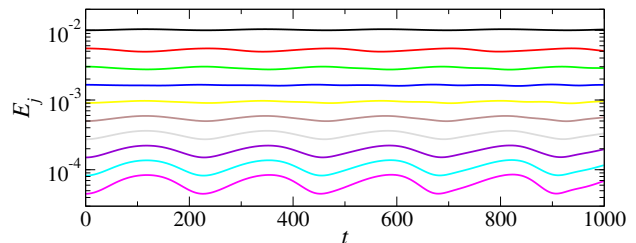


FIG. 2. Energy per mode for $0 \leq j \leq 9$ for TTF solution with initial data $A_j(0) \propto \exp(-0.3j)/(2j+3)$.

We consider initial data $A_j(0) = \epsilon \exp(-\mu j)/(2j+3)$, which well-approximates $j_r = 0$ quasi-periodic solutions. Varying μ and also adding random perturbations, we observe periodic oscillations about the quasi-periodic solution, providing evidence for stability (see Fig. 2). For smaller values of μ , energy levels are more closely spaced, resulting in more rapid energy transfers between modes, leading to larger-amplitude oscillations. Likewise, larger random perturbations increase the amplitude of oscillation, as the initial data deviates more strongly from a quasi-periodic solution. Results from TTF and full numerical relativity simulations are in close agreement.

Two-mode initial data.—Our main interest is to understand which initial conditions can be expected to collapse. Thus it is necessary to study initial data that are *not* expected to closely approximate a quasi-periodic solution. A particularly interesting case consists of two modes initially excited (all others zero) as this case was key to the argument of [5] showing the onset of the turbulent cascade. In contrast to results of the previous section, two-mode initial data,

$$A_j(0) = \frac{\epsilon}{3} (\delta_j^0 + \kappa \delta_j^1), \quad (20)$$

involves considerable energy transfer among modes provided κ is sufficiently large. [For $\kappa \ll 1$, (20) may be considered as a perturbation about single-mode data.] We examined several choices of κ using both TTF and full numerical relativity, with similar results. Here we restrict to $\kappa = 3/5$ —the equal-energy case.

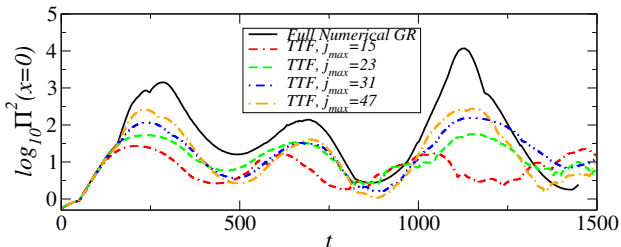


FIG. 3. Full numerical and TTF results for 2-mode equal-energy initial data with $\epsilon = 0.09$. As j_{\max} is increased, the TTF solutions achieve better agreement with the full numerics. Recurrence behavior observed in the full numerical solution is reasonably well captured by TTF.

The upper envelope of $\Pi^2(x=0)$ is often used as an indicator of the onset of instability [5, 7, 11]. We plot this quantity in Fig. 3, both for full GR simulations and TTF solutions with varying j_{\max} . In the full GR simulation, $\Pi^2(x=0)$ grows initially, but, in contrast to blowup observed in [5] for Gaussian scalar field profile, it then decreases close to its initial value. This *recurrence* phenomenon repeats and—for sufficiently small ϵ —collapse never occurs for as long as we have run the simulation. Recurrence was also observed in previous work [11] for broadly distributed Gaussian profiles.

Also in Fig. 3, TTF solutions appear to converge to the full numerical GR solution as j_{\max} is increased. (Strictly speaking, the TTF and numerical approaches converge as both $j_{\max} \rightarrow \infty$ and $\epsilon \rightarrow 0$; see the accompanying supplemental material for more discussion.) This illustrates nicely the cascade/collapse mechanism: Higher- j modes are more sharply peaked at $x=0$, so as the (conserved) energy is transferred to these modes, $\Pi^2(x=0)$ attains higher values. Truncating the system at finite j_{\max} artificially places a bound on values of $\Pi^2(x=0)$ that can be reached. In particular, $\Pi^2(x=0)$ can never blow up for $j_{\max} < \infty$.

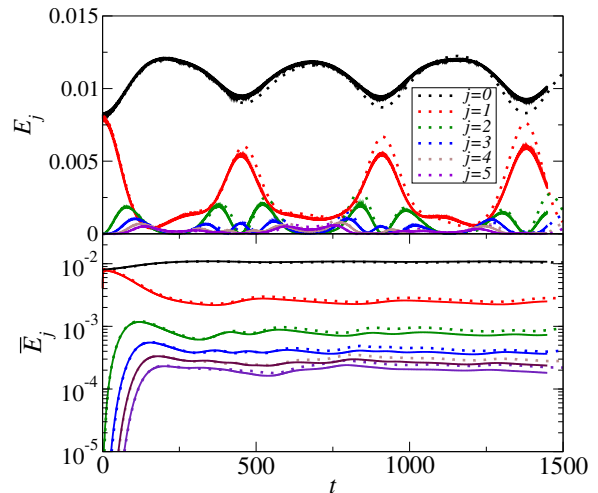


FIG. 4. Full numerical (solid) and TTF (dotted) energy (top panel) and running time-average energy (bottom panel) per mode, for 2-mode equal-energy initial data. Notice the repeated approximate return of the initial energies to the first two modes in the top panel and the running time-average energies asymptoting to distinct values. For this run with $j_{\max} = 47$, $\sum_{j=0}^{11} |E_j^{\text{TTF}} - E_j^{\text{numerical}}| / E^{\text{total}}$ does not exceed 0.19. For $j_{\max} = (31, 23, 15)$ the bounds are (0.28, 0.42, 0.57). (The horizontal offset is partially attributed to a slight difference in time-normalization for our numerical and TTF codes.)

It is useful to examine the solution mode by mode, and in Fig. 4 we show the energy per mode as a function of time. Initially, energy is distributed evenly between modes $j=0, 1$. It then flows out of $j=1$ to mode $j=2$, then $j=3$, etc. At some point in time, energy begins to flow *back* to mode $j=1$ —an *inverse energy cascade*. By $t \approx 450$ the state has nearly returned to the original configuration. This recurrence behavior then repeats.

The bottom plot of Fig. 4 illustrates the running time-average energy per mode $\bar{E}_j(t) \equiv t^{-1} \int_0^t E_j(t') dt'$. Rather than cascading to ever-higher modes, the energy sloshes primarily between low- j modes, in a “metastable” state. We never observe thermalization, *i.e.*, no equipartition of energy occurs.

Fig. 4 is remarkably similar in appearance to plots of FPUT [12] (cf. Figs. 4.1 and 4.2 of [15].) FPUT numerically simulated a collection of nonlinearly coupled harmonic oscillators and expected to see thermalization. Instead, they observed the same recurrence we see here. Indeed, as the TTF formulation (17) of our system makes clear, small-amplitude scalar collapse in AdS reduces precisely to a (infinite) set of nonlinearly coupled oscillators, so the similar behavior should not be surprising. More precisely, our system is related to the FPUT β -model [15]. (Of course, the particular resonances and nonlinear interactions differ between our system and FPUT.) Predicting when the FPUT system of oscillators thermalizes is a longstanding problem in nonlinear dynamics, and is

indeed known as the FPUT *paradox* [15–17].

Discussion.—Common intuition suggests that a finite-sized strongly interacting system driven off-equilibrium, even by a small amount, eventually thermalizes. This thermalization would imply, via AdS/CFT, that arbitrarily small perturbations about global AdS *must* result in gravitational collapse. However, we have uncovered in this Letter a large class of initial conditions for a massless, self-gravitating real scalar field in AdS₄, that *fail* to collapse. We constructed and evolved these initial conditions within a newly proposed TTF, as well as through full numerical GR simulations. TTF shows that scalar perturbations of AdS are in the same universality class as the famous FPUT problem [12]. Thus, perturbed AdS spacetimes act as a holographic bridge between non-equilibrium dynamics of CFTs and the dynamics of nonlinearly coupled oscillators and the FPUT paradox. In this Letter we focused on the dynamics of low-energy 2+1 dimensional CFT excitations “prepared” with nonzero expectation values of dimension three (marginal) operators. Extensions to higher-dimensional CFTs, as well as to states generated by (ir)relevant operators are straightforward.

Acknowledgments: We would like to thank A. Polkovnikov and J. Santos for interesting discussions and correspondence. We also thank D. Minic and A. Zimmerman for pointing us to the FPUT problem. Finally, we thank P. Bizon and A. Rostworowski for discussions and direct comparison of numerical solutions. This work was supported by the NSF under grants PHY-0969827 & PHY-1308621 (LIU), NASA under grant NNX13AH01G, NSERC through a Discovery Grant (to A.B. and L.L.) and CIFAR (to L.L.). S.R.G. acknowledges support by a CITA National Fellowship. L.L. and S.L.L. also acknowledge the Centre for Theoretical Cosmology at the University of Cambridge for their hospitality and its participants for helpful discussions at the “New Frontiers in Dynamical Gravity” meeting during which this work was completed. Research at Perimeter Institute is supported through Industry Canada and by the Province of Ontario through the Ministry of Research & Innovation. Computations were performed at Sharnet.

- land, B. Craps, *et al.*, Phys. Rev. Lett. **106**, 191601 (2011), arXiv:1012.4753 [hep-th].
- [4] A. Buchel, R. C. Myers, and A. van Niekerk, Phys. Rev. Lett. **111**, 201602 (2013), arXiv:1307.4740 [hep-th].
- [5] P. Bizon and A. Rostworowski, Phys. Rev. Lett. **107**, 031102 (2011), arXiv:1104.3702 [gr-qc].
- [6] M. Maliborski and A. Rostworowski, Phys. Rev. Lett. **111**, 051102 (2013), arXiv:1303.3186 [gr-qc].
- [7] A. Buchel, L. Lehner, and S. L. Liebling, Phys. Rev. **D86**, 123011 (2012), arXiv:1210.0890 [gr-qc].
- [8] M. Maliborski and A. Rostworowski, (2014), arXiv:1403.5434 [gr-qc].
- [9] O. J. Dias, G. T. Horowitz, D. Marolf, and J. E. Santos, Class. Quant. Grav. **29**, 235019 (2012), arXiv:1208.5772 [gr-qc].
- [10] J. Abajo-Arrostia, E. da Silva, E. Lopez, J. Mas, and A. Serantes, (2014), arXiv:1403.2632 [hep-th].
- [11] A. Buchel, S. L. Liebling, and L. Lehner, Phys. Rev. **D87**, 123006 (2013), arXiv:1304.4166 [gr-qc].
- [12] E. Fermi, J. Pasta, and S. M. Ulam, *Studies of nonlinear problems. I*, Technical Report LA-1940 (1955) also in *Enrico Fermi: Collected Papers, volume 2*, edited by Edoardo Amaldi, Herbert L. Anderson, Enrico Persico, Emilio Segré, and Albedo Wattenberg. Chicago: University of Chicago Press, 1965.
- [13] T. Dauxois, Physics Today **61**, 010000 (2008), arXiv:0801.1590 [physics.hist-ph].
- [14] J. Kevorkian and J. D. Cole, *Multiple scale and singular perturbation methods*, Applied mathematical sciences, Vol. 114 (Springer, New York, 1996).
- [15] G. Benettin, A. Carati, L. Galgani, and A. Giorgilli, *The Fermi-Pasta-Ulam Problem and the Metastability Perspective*, Lecture Notes in Physics, Vol. 728 (Springer, Berlin, 2008).
- [16] P. Poggi, S. Ruffo, and H. Kantz, Phys. Rev. E **52**, 307 (1995).
- [17] G. P. Berman and F. M. Izrailev, Chaos **15**, 015104 (2005), nlin/0411062.

* vbalasu8@uwo.ca

† abuchel@perimeterinstitute.ca

‡ sgreen04@uoguelph.ca; CITA National Fellow

§ llehner@perimeterinstitute.ca

¶ steve.liebling@liu.edu

- [1] O. Aharony, S. S. Gubser, J. M. Maldacena, H. Ooguri, and Y. Oz, Phys. Rept. **323**, 183 (2000), arXiv:hep-th/9905111 [hep-th].
- [2] P. M. Chesler and L. G. Yaffe, Phys. Rev. Lett. **102**, 211601 (2009), arXiv:0812.2053 [hep-th].
- [3] V. Balasubramanian, A. Bernamonti, J. de Boer, N. Cop-

Holographic Thermalization, stability of AdS, and the Fermi-Pasta-Ulam-Tsingou paradox:

Supplementary Material

Venkat Balasubramanian,^{1,*} Alex Buchel,^{1,2,†} Stephen R. Green,^{3,‡} Luis Lehner,^{2,§} and Steven L. Liebling^{4,¶}

¹*Department of Applied Mathematics, University of Western Ontario, London, Ontario N6A 5B7, Canada*

²*Perimeter Institute for Theoretical Physics, Waterloo, Ontario N2L 2Y5, Canada*

³*Department of Physics, University of Guelph, Guelph, Ontario N1G 2W1, Canada*

⁴*Department of Physics, Long Island University, Brookville, NY 11548, U.S.A*

Summary.—We provide additional description of the approximations involved in TTF, as well as expectations for convergence in both ϵ and j_{\max} to full general relativity. Last, we present results of tests validating our full GR code.

Approximations.—As described in our Letter, TTF involves two approximations: small ϵ and truncation in mode number j . By working to $O(\epsilon^3)$ we neglect interactions of higher than cubic order in metric perturbations, but we keep the lowest order nontrivial interactions. This gives rise to an infinite set of coupled oscillons, which in practice must be truncated at a finite mode number $j = j_{\max}$. We were able to explicitly determine the equations up to $j_{\max} = 47$.

Small ϵ .—The TTF equations possess a scaling symmetry, $A_j(\tau) \rightarrow \epsilon A_j(\tau/\epsilon^2)$. The full Einstein equation does not possess this symmetry, however, and it is evident that had we included higher order in ϵ interactions in TTF, they would break the scaling symmetry. The presence of the scaling symmetry in a set of solutions to the full Einstein equation therefore indicates that higher order in ϵ interactions are negligible for these solutions. In Fig. 1 we plot the upper envelope over rapid oscillations of $\Pi^2(x=0)$ for full numerical solutions obtained with several values of ϵ for 2-mode equal-energy initial data, as well as a plot of rescaled values. It is clear that these solutions *do* possess an approximate scaling symmetry for sufficiently small ϵ (see also Fig. 2 of [1]).

Initial data for Fig. 1 is the same (up to overall normalization) as that of Figs. 3 and 4 of the Letter. Because of the approximate scaling symmetry in Fig. 1, the discrepancy between TTF and full GR in Fig. 3 of the Letter is therefore primarily attributed to truncation in mode number j . In addition, as ϵ is decreased, comparison of Fig. 1 and Fig. 3 of the Letter reveals that the small degree of non-scaling of the full GR solution brings it into closer agreement with TTF.

Mode number truncation.—For 2-mode equal-energy initial data, under evolution the majority of the energy remains in the lowest- j modes (see Fig. 4 of the Letter). Nevertheless, $\Pi^2(x=0)$ can become very peaked. This is because higher- j modes are more sharply peaked about the origin. Even small amounts of energy in high- j modes can lead to growth of $\Pi^2(x=0)$, despite the dynamics being dominated by low- j modes. This property can lead to

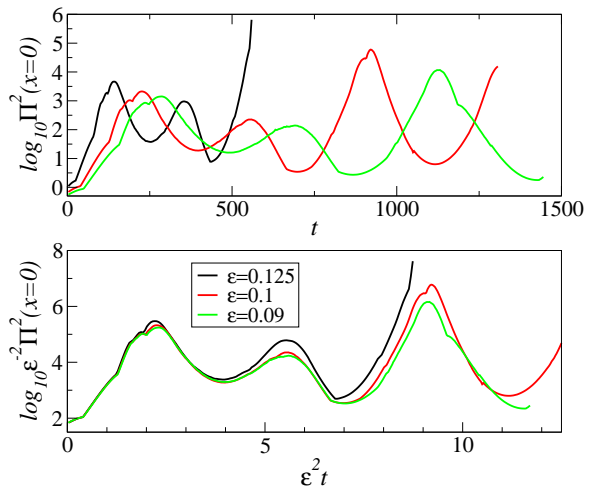


FIG. 1. (Color online) Full numerical GR solutions for 2-mode equal-energy initial data for different values of ϵ . The bottom plot shows the same data, appropriately rescaled in time and amplitude by ϵ . The $\epsilon = 0.125$ case collapses to black hole at $t \approx 550$. However, for smaller ϵ black hole formation is avoided with an inverse cascade. As ϵ increases and collapse to black hole ensues, the scaling symmetry in ϵ is broken as higher order terms (above third order) become important.

collapse in the case where sufficient energy is transferred to high- j modes (*e.g.*, Gaussian initial data in [1]).

We have attempted to show in Fig. 3 of the Letter that increasing j_{\max} gives rise to a better approximation of the full solution. This is best illustrated at early times, before the higher modes are populated, in which case the lack of available higher modes in a truncated TTF system is irrelevant. However, once the truncation begins to affect the dynamics, the overall solution is altered and it is more difficult to compare with full GR. Nevertheless, it is clear throughout the simulation that for higher j_{\max} , larger values of $\Pi^2(x=0)$ can be attained.

This discussion and the accompanying figures support the assertions that: (i) the TTF and the fully nonlinear solutions converge as $j_{\max} \rightarrow \infty$ and $\epsilon \rightarrow 0$, and (ii) the level to which the nonlinear solutions scale improves with decreasing ϵ .

The truncated TTF equations are able to accurately model the dynamics of low- j modes for the 2-mode data,

as shown in Fig. 4 of the main paper. However, the exact solution involves excitations of very high mode numbers at the peaks of $\Pi^2(x=0)$, and the TTF equations with $j_{\max} = 47$ are not sufficient to match the fully nonlinear result. However, we can instead consider a case where we expect better agreement. To that end, we include in Fig. 2 a plot of the full numerical GR and TTF solutions for an initially exponential energy spectrum. This solution is (a) close to a quasi-periodic solution, and (b) has very little energy in high- j modes. In particular, the exponential fall-off in the energy spectrum with j overwhelms the polynomial growth in peakiness about $x=0$. Thus in this case, the truncated TTF and full numerical GR are in very close agreement¹.

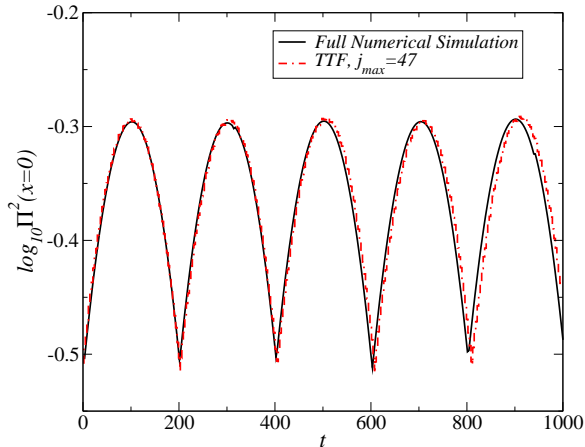


FIG. 2. (Color online) Full numerical GR and TTF solutions for initial data $A_j(0) = 0.05 \exp(-j)/(2j+3)$ which approximates a quasi-periodic solution.

Full numerical GR code validation.—The code we use has been described and thoroughly tested in [2, 3] to study scalar collapse in AdS. In particular we have confirmed: convergence of the obtained solutions with increased resolution, mass conservation, and convergence to zero of the constraint residuals (similar to Fig. 3 of [2]).

We present another, longer example of such a convergence study in Fig. 3. The results unambiguously indicate a convergent code over a large number of dynamical timescales (roughly $600/\pi \approx 190$). The test also directly confirms that, while a direct cascade dominates at early times, the system exhibits both direct and inverse cascades that compete with each other, a central result of

this Letter; note in the bottom panel that the three highest resolutions have essentially converged to such a transition at $t \approx 230$.

This test also helps understand the failure of the TTF in Fig. 3 of the Letter to resolve the first peak of $\Pi^2(0, t)$. As mentioned previously, the TTF simply cannot resolve energy in high frequency modes compared to j_{\max} . Even the fully nonlinear code must extend to very high resolutions to resolve it spatially. Nevertheless, as indicated in Fig. 4 of the Letter and in Fig. 2 of this supplement, the TTF captures the essential dynamics of the system and matches the behavior of the fully nonlinear evolutions for the low frequency modes.

This study tests evolutions with a single grid-spacing, but in practice we use adaptive mesh refinement (AMR) to greatly reduce computational overhead. With an AMR code such as ours, one can vary a number of parameters to increase the effective resolution, and we often increase both the resolution of the base grid as well the criterion for refinement. We verify that such changes do not produce different results (see Figs. 5 and 6 of Ref. [3] for past examples of tests of our AMR code). In particular, AMR results are consistent with unigrid results that show a series of direct and indirect cascades (see Fig. 4).

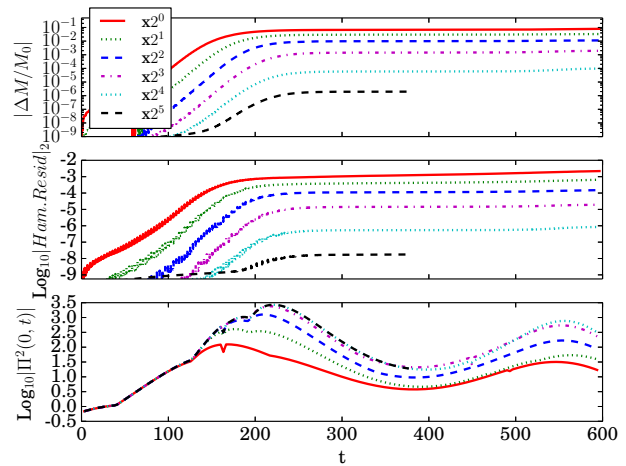


FIG. 3. (Color online) Demonstration of convergence for unigrid evolutions of equal-energy, two-mode initial data with $\epsilon = 0.1$. Shown for subsequent doublings of resolution are: (top) total mass loss, (middle) norm of the residual of the Hamiltonian constraint, and (bottom) the value of $\Pi^2(0, t)$. Note that the top panels display a measure of the error which progressively diminishes with resolution, indicating convergence. The bottom panel displays a feature of the evolution and quickly approaches a unique solution consistent with convergence. The base resolution (red, solid line) uses $316 + 1$ points while the highest resolution (black, dashed line) uses $10,112 + 1$ points.

¹ The horizontal offset in Fig. 2 (and Figs. 3 and 4 of the Letter) between TTF and full numerical GR is attributed to a small difference in time-normalization between our codes. Specifically, the full numerical GR code sets $\delta = 0$ at the AdS boundary, whereas the TTF equations set $\delta = 0$ at $x = 0$. This gauge freedom amounts to a difference in time-normalization. The first nonzero contribution to δ is at $O(\epsilon^2)$, so this is a small effect.

As a final comment we note that in keeping with Ref. [4], we refer to the famous FPUT paradox within the

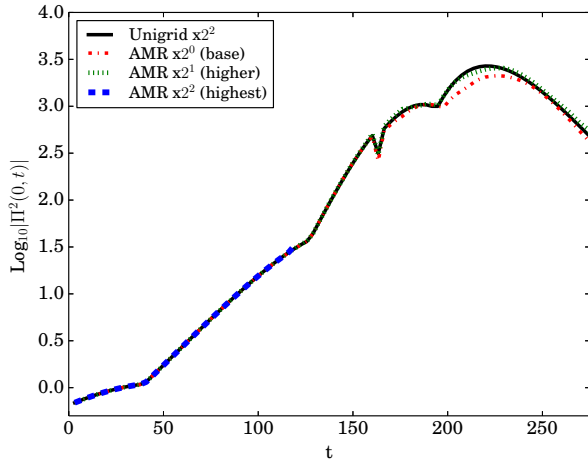


FIG. 4. (Color online) Demonstration of convergence for AMR evolutions of equal-energy, two-mode initial data with $\epsilon = 0.1$. Shown is the value of $\Pi^2(0, t)$ for three different AMR resolutions as well as the highest unigrid result from Fig. 3. Each successive AMR evolution uses a base grid with twice the resolution and a smaller threshold for refinement. The highest resolution AMR result has the same base resolution as the unigrid result.

main text by all four names of the contributors, Fermi, Pasta, Ulam, and Tsingou (later Menzel).

* vbalasu8@uwo.ca

† abuchel@perimeterinstitute.ca

‡ sgreen04@uoguelph.ca; CITA National Fellow

§ lehner@perimeterinstitute.ca

¶ steve.liebling@liu.edu

- [1] P. Bizon and A. Rostworowski, Phys. Rev. Lett. **107**, 031102 (2011), arXiv:1104.3702 [gr-qc].
- [2] A. Buchel, L. Lehner, and S. L. Liebling, Phys. Rev. **D86**, 123011 (2012), arXiv:1210.0890 [gr-qc].
- [3] A. Buchel, S. L. Liebling, and L. Lehner, Phys. Rev. **D87**, 123006 (2013), arXiv:1304.4166 [gr-qc].
- [4] T. Dauxois, Physics Today **61**, 010000 (2008), arXiv:0801.1590 [physics.hist-ph].